Steel and Composite Structures, *Vol. 21, No. 2 (2016) 357-371*
DOI: http://dx.doi.org/10.12989/scs.2016.21.2.357

Shear behavior of exposed column base connections

Yao Cui*

State Key Laboratory of Coastal and Offshore Engineering, School of Civil Engineering, Dalian University of Technology, No. 2 Linggong-road, Dalian 116024, P.R. China

(*Received February 03, 2016, Revised April 01, 2016, Accepted April 05, 2016*)

Abstract. Column base connections are critical components in steel structures because they transfer axial forces, shear forces and moments to the foundation. Exposed column bases are quite commonly used in low- to medium-rise buildings. To investigate shear transfer in exposed column base plates, four large scale specimens were subjected to a combination of axial load (compression or tension) and lateral shear deformations. The main parameters examined experimentally include the number of anchor rod, arrangement of anchor rod, type of lateral loading, and axial force ratio. It is observed that the shear resisting mechanism of exposed column base changed as the axial force changed. When the axial force is in compression, the resisting mechanism is rotation type, and the shear force will be resisted by friction force between base plate and mortar layer. The specimens could sustain inelastic deformation with minimal strength deterioration up to column rotation angle of 3%. The moment resistance and energy dissipation will be increased as the number of anchor rods increased. Moreover, moment resistance could be further increased if the anchor rods were arranged in details. When the axial force is in tension, the resisting mechanism is slip type, and the shear force will be resisted by the anchor rods. And the shear resistance was reduced significantly when the axial force was changed from compression to tension. The test results indicated that the current design approach could estimate the moment resistance within reasonable acceptance, but overestimate the shear resistance of exposed column base.

Keywords: exposed column base; anchor rods; shear behavior; hysteretic behavior; axial force ratio

1. Introduction

Steel moment resisting frames and braced frames are commonly used in seismic regions. The column base has significant effects on the behavior and performance of these frames. The column base is commonly classified into two types: (1) the exposed column base that consists of a steel base plate welded to the end of the column and anchor rods that connect the base plate to a reinforced concrete (RC) foundation beam; and (2) the embedded column base where the column is embedded in a RC foundation. Although the embedded column base is greater in fixity against rotation than is the exposed column base, the exposed column base has been popularly used for low- to medium-rise structures because of better constructability and low cost.

Column base connections are critical components in steel structures because they transfer axial forces, shear forces and moments to the foundation. In the U.S., publications such as DeWolf (1982), Thambiratnam and Paramasivam (1986), and the AISC Design Guide No. 1 (Fisher and

*Corresponding author, Ph.D., E-mail: cuiyao@dlut.edu.cn

http://www.techno-press.org/?journal=scs&subpage=6 ISSN: 1229-9367 (Print), 1598-6233 (Online)

Koliber 2006) are commonly used as guidelines for the design of exposed column bases. Design provisions have been offered, for instance, AISC Manual of Steel Construction (AISC 2005b), and AISC Seismic Provisions (AISC Seismic 2005a) in the U.S, the ENV1993 Eurocode 3 (ENV or EuroNormVornorm, represents a European pre-standard) (CEN 1992) in Europe, and Recommendation for Design of Connections in Steel Structures (AIJ 2006) in Japan.

So far, there are large numbers of research on the seismic behavior of exposed column base under complex stress condition (Akiyama 1985, Sato 1987, Grauvilardell *et al*. 2005, Demir *et al*. 2014). For example, studies on the effect of the base plate thickness on the column base behavior (DeWolf 1982, Astaneh *et al*. 1992), the effect of the base plate size on ductility (Burda and Itani 1992), the seismic performance of exposed column base (Kanvinde *et al*. 2012), and the rotational stiffness of exposed column base (Stamatopoulos and Ermpoulos 2011, Kanvinde *et al*. 2015). Chi and Liu (2012) developed the post-tensioned column base which could reduce the residual drift of the steel frame under earthquake, Borzouie *et al*. (2016) developed an asymmetric friction connection at the column base, which exhibited low-damage performance under earthquake.

However, relatively limited research focus on the behavior of exposed column under shear force compared with the behavior of exposed column base under bending moment. Recent studies by Grauvilardel *et al*. (2005) and Cui *et al*. (2015) indicate that in structural systems such as braced frames, a base plate connection may experience extremely large shear-to-moment ratios, such that failure of the connection is dominated by shear.

Exposed column base resisted shear force by the friction between base plate and mortar layer, anchor rod bearing, shear key bearing and direct contact of base plate to foundation concrete. Fig. 1 illustrated the shear resisted mechanism of exposed column base. Experimental research of shear transfer in base plates has not been explicitly addressed, although the associated mechanisms, e.g., surface friction (Rabbat and Russel 1985, Nagae *et al*. 2006) or anchor rod failure (Burdette 1987, Cook and Klingner 1992, Ai *et al*. 2012) or shear key failure (Rotz and Reifschneider 1989, Xiao *et al*. 2010), have been researched in separate contexts. Thus, current design provisions for base plates typically adapt and combine findings from several of these studies, which rely on small-scale component tests of specific failure mechanisms (e.g., pullout or shear tests of individual anchor rods).

Therefore, there is a lack of data involving large scale base plate components, where various mechanisms may interact with each other or may be influenced by the construction procedures or geometry of the base connection itself. Moreover, few studies examine the effect of cyclic loading on base plate shear transfer details, which is important from the perspective of seismic design. The

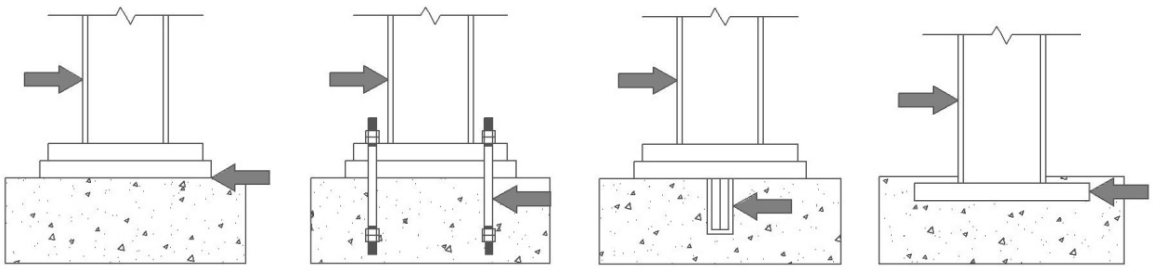

(a) Surface friction (b) Anchor rod bearing (c) Shear-key bearing (d) Direct contact

Fig. 1 Column bases loaded by shear force

primary motivation of this paper is to investigate the seismic behavior and failure modes of exposed column base connections under shear loading. The unique behavior of column base under shear-dominated loading will be investigated in details based on a series of experiments.

2. Experimental study

2.1 Test specimens

Four exposed column base specimens were tested. Fig. 2(a) shows the geometry of the specimen. The specimen comprises a steel column and a concrete beam. The column is a square-tube cross section having the width of 200 mm and the thickness of 12 mm. The height from the base plate to the top of the steel column is 560 mm to ensure large shear-to-moment ratio. The base plate is 350 mm × 350 mm and 40 mm in thickness. The concrete foundation beam was reinforced well to ensure damage will concentrate on the anchor rods rather than concrete foundation beam. Steel Q235 (f_y = 235 MPa) was used for both column and base plate. According to the design manual of steel structure connections (JSSC 2009), the thickness of mortar layer between base plate and foundation beam is 40 mm. M20 anchor rod was used, the material is Steel Q235, and the embedded length of anchor rod is 400 mm.

The arrangement of anchor rod is shown in Fig. 2(b). The distance between anchor rods is 260 mm in both directions for "Type a" arrangement. For the other two type arrangement, one more anchor rod is added either in the sides along loading direction or the sides perpendicular to the loading direction. The geometry of the specimens is shown in Fig. 2 and the main parameters of specimens are listed in Table 1.

Specimen 4Q was designed as prototype. One specimen, specimen 4QT, was loaded under tensile axial force (axial force ratio is -0.1) and the other three specimens, specimens 4Q, 6CQ, and 6EQ, were loaded under compressive axial force (axial force ratio is 0.2). Specimens 6EQ

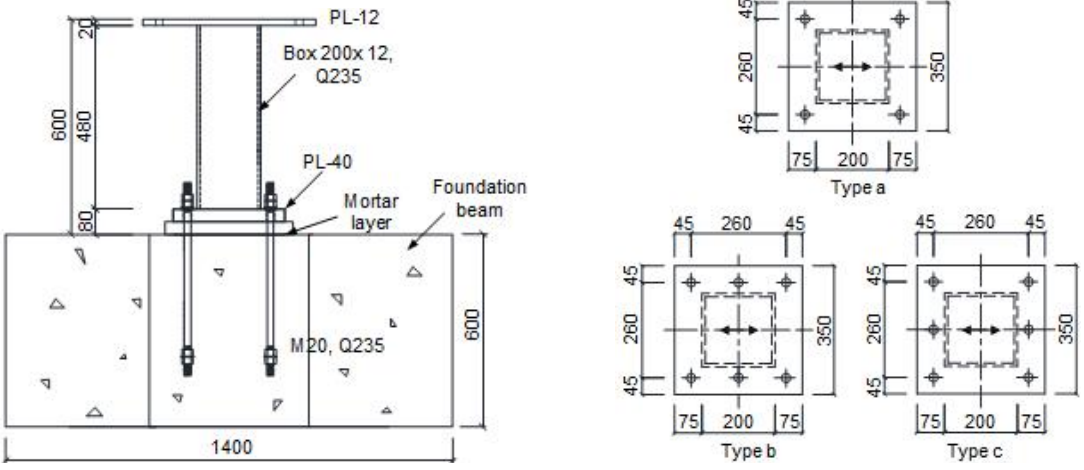

(a) Geometry of specimen (b) Arrangement of anchor rods

Fig. 2 Test specimens (unit: mm)

Table 1 Parameters of specimens

Specimen	Axial force P (kN)	Num. of anchor rod	Anchor rod arrangement
4Q	540 (compression)	4	Type a
4QT	-270 (tension)	4	Type a
6EQ	540 (compression)	6	Type b
6CQ	540 (compression)	6	Type c

Table 2 Material properties

		Yield stress, σ_y (N/mm^2)	Tensile stress, σ_u (N/mm^2)
Column	□-200×12, Q235	373	486
Anchor rod	M20, Q235	276	435

and 6CQ were designed to investigate the effect of the number of anchor rods, as shown in Fig. 2(b). The arrangements of anchor rods were also different. Material properties of each part are listed in Table 2.

2.2 Test setup

The test specimen was placed in the loading frame shown in Fig. 3. The foundation beam was clamped to the reaction floor. The column top was clamped to two hydraulic jacks, one in the horizontal direction and the other in the vertical direction. The specimens 4Q, 6CQ, 6EQ was subjected to a constant vertical force of 540 kN, corresponding to 0.2 times the yield axial load of the column (12 mm thick). While, the specimen 4QT was subjected to a constant vertical tensile force of 270 kN, corresponding to 0.1 times of the yield axial load of the column. A displacement-controlled cyclic load was applied quasi-statically in the horizontal direction. The loading was controlled by the rotation of a column specimen calculated as the horizontal displacement at the loading point relative to the height of the column. The loading rotation angles of 0.0005, 0.005, 0.01, 0.02, 0.03, 0.04, 0.06, 0.08, and 0.1 rad were adopted, and two cycles were performed at each level. The test was terminated when the loading rotation angle reached 0.1 rad or two of the anchor rods fractured, which was regarded as a complete failure.

The locations of the displacement transducers are shown in Fig. 4(a). Two wire-type displacement transducer one (D1) oriented in the horizontal direction and the other (D2) oriented in vertical direction, measured the deformations of the test specimens. Six high-sensitivity displacement transducers were set to measure the sliding (D3-4) and rotations (D5-8) of the welded base plate to the column bottom. One displacement transducer (D9) was set to measure the sliding of the test specimens.

To measure the strains of anchor rods, strain gauges were glued as shown in Fig. 4(b). Eight strain gauges were applied on each side of the anchor rods at distances of 0, 90, 180 and 270 mm respectively measured from the top surface of concrete foundation. Four strange gauges were glued on the column to monitor the yield behavior of column. The strain gauges were applied on each side of the column flange at a distance of 90 mm measured from the top surface of baseplate, as shown in Fig. 4(b).

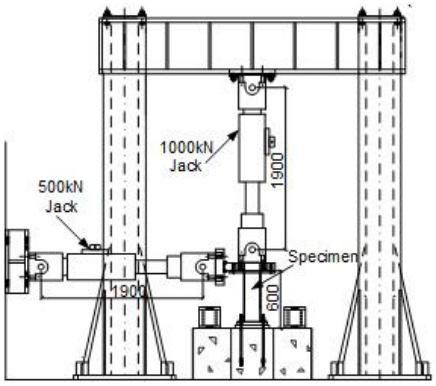

Fig. 3 Test setup (unit: mm)

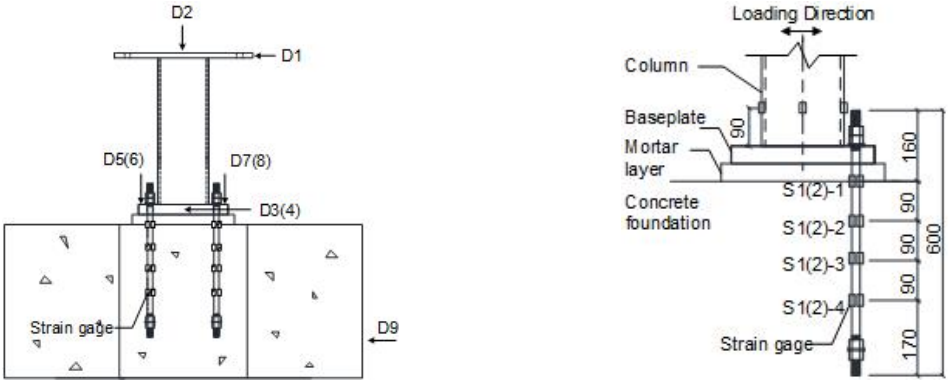

(a) Arrangement of displacement transducer (b) Arrangement of strain gages

Fig. 4 Instrumentations

3. Test results

3.1 Failure modes

In this test, the specimens were loaded from 0 to 0.1 rad column rotation angle, which was calculated by considering the geometrical relations of the loading point. According to the strain gage attached on the column, the column was not yielded. All the damage was occurred at the joint area between base plate and mortar layer, as shown in Fig. 5.

Three specimens under compression axial load were tested till the column rotation angle of 0.1 rad was reached. The specimen under tensile axial load (specimen 4QT) was stopped at the second loading cycle of column rotation angle of 0.04 rad. Fig. 5 showed the deformation of column base at the ultimate strength. It is noted that in specimen 4QT the base pate was completely separated from the mortar layer, and the anchor rods were elongated significantly in comparison with other specimens. In these four specimens, only anchor rods of specimen 4QT were fracture. The anchor rods of the other three specimens showed good ductility.

The failure modes were two types depends on the axial force. For the specimens with axial force ratio of 0.2 (specimen 4Q, 6CQ, and 6EQ), anchor rods yielded at 3% column rotation angle

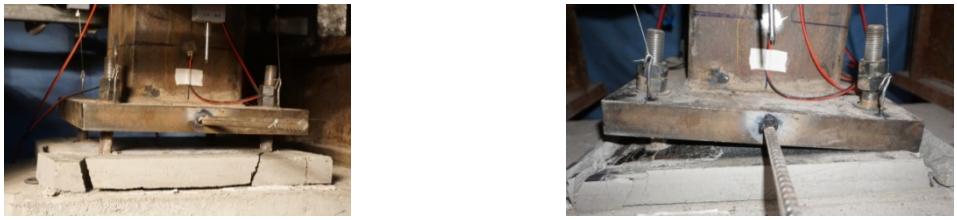

(a) 4QT (b) 4Q

(c) 6CQ (d) 6EQ

Fig. 5 Deformation of specimens at the ultimate load

and showed good ductility after yielding. Moreover, the anchor rods were not fractured even the column rotation angle reached 0.1 rad. For the specimens with axial force ratio of -0.1 (specimen 4QT), anchor rod was fractured at 0.04 rad column rotation angle.

The base plate of specimen 4Q, 6CQ, and 6EQ rotated around the anchor rod in the compression side as the displacement of column top increased. Therefore, the anchor rods in the tension side were elongated, as shown in Fig. 4. During the loading, there always is part of the base plate contacted with mortar layer of concrete foundation beam. Therefore, the shear force could resist by the friction between the base plate and mortar layer. It is the same as the shear mechanism as shown in Fig. 1(a).

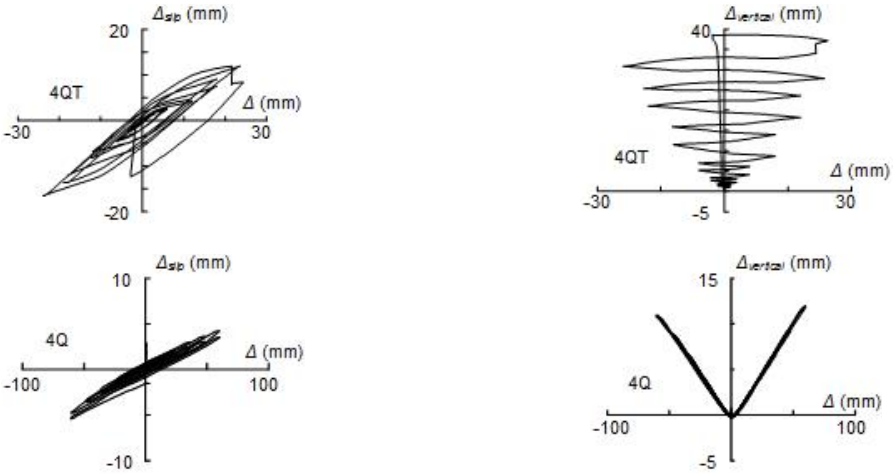

(a) Horizontal direction (b) Vertical direction

Fig. 6 Displacement of base plate

(a) Rotation type (b) Slip type

Fig. 7 Shear resistance mechanism of exposed column base

The base plate of specimen 4QT was separated from the foundation beam during the loading. Different from the specimens with 0.2 axial force ratio, specimen 4QT exhibited slip behavior rather than rotation behavior. Till the end of loading, anchor rods showed shear deformation, as shown in Fig. 5.

The horizontal and vertical displacement of the base plate of specimen 4QT and 4Q are compared in Fig. 6. As shown in Fig. 6(a), the horizontal displacement of base plate increased as the displacement of column top increased, till the end of loading (0.04 rad column rotation) the horizontal displacement is 25 mm, which is about 60% of the total deformation of the specimen for specimen 4QT. For specimen 4Q, the maximum horizontal displacement (around 5 mm) of base plate was reached at the end of loading (0.1 rad column rotation), and it is far smaller than the horizontal displacement of specimen 4QT. As shown in Fig. 6(b), the vertical displacement of specimen 4QT increased as the loading increased. It means the anchor rods of specimen 4QT were elongated and base plate was separated from the foundation beam. Therefore, specimen 4QT resisted shear force by the anchor rods bearing (Fig. 1(b)) instead of the friction (Fig. 1(a)).

Under axial force, bending moment and shear forces, exposed column base will rotate and slip simultaneously. According to the axial load, the shear resistance mechanism of exposed column base could be rotation type or slip type, as shown in Fig. 7. When the axial force is in compression and relatively large, the shear resistance mechanism of column base will be rotation type (Fig. 7(a)). The exposed column base will resist shear force mainly by friction. The base plate will rotate around the anchor rods in compression side, and the anchor rod in tension side will resist both tension and bending. When the axial force is in tension or relatively small in compression, the shear resistance mechanism of column base will be slip type, as shown in Fig. 7(b). The exposed column base will resist shear force mainly by anchor rods. The base plate will separate from the foundation beam. All the anchor rods resist both tension and shear.

3.2 Hysteresis curves

Figs. 8(a) and (b) showed the shear force and lateral displacement of the four specimens. In Fig. 8(a), the horizontal axis represents the total lateral displacement (Δ) including the slip of baseplate (Δ_{slip}) and the lateral displacement of column (Δ_{rot}). And in Fig. 8(b), the horizontal axis represents the lateral displacement of column (Δ_{rot}).

Specimen 4QT failed at column rotation angle of 0.04 rad. The fracture point was indicated in Fig. 8. Compared with the prototype specimen 4Q, the shear strength of specimen 4QT reduced

around 70%. And the shape of hysteresis curves of specimen 4QT are different with the other three specimens. The hysteresis curves of the other three specimens (specimen 4Q, 6CQ, and 6EQ) in pinched, and the shear resistance returned to zero when the specimens were unloaded. In contrast, specimen 4QT exhibited some residual displacement when it was unloaded. From Figs. 8(a) and (b), it could be noted that the slip of specimen 4QT is relatively larger than the other three specimens. The lateral displacement of column (Δ_{rot}) which is contributed by the column rotation is less than 50% for specimen 4QT and it is about 90% for the other three specimens.

Moment-rotation curve could represent the rotation behavior of the specimens. In Fig. 8(c), the horizontal axis represents the column rotation angle, the vertical axis represents the resisting moment at the base plate. When axial force ratio is -0.1 (axial force is 270 kN in tension), the hysteresis curve is different from the others. The moment of specimen 4QT is significantly smaller than the other three specimens. According the strain gage data, the anchor rods in tension side yielded when the column rotation is 0.005 rad. When the column rotation is 0.04 rad, the maximum moment was reached. Anchor rods in tension side were suddenly fractured in the second loading of 0.04 rad. The moment was reduced quickly and the loading was ended.

When the axial force ratio is 0.2 (axial force is 540 kN in compression), the hysteresis curve is pinched as described in previous studies (Akiyama 1985, Sato 1987, Cui *et al*. 2009). The yielded moment was controlled by the anchor rods in tension side. According the strain gages attached

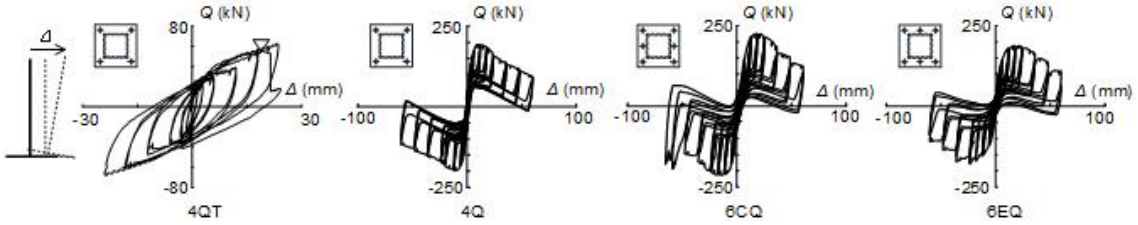

(a) Shear force - lateral displacement relationship

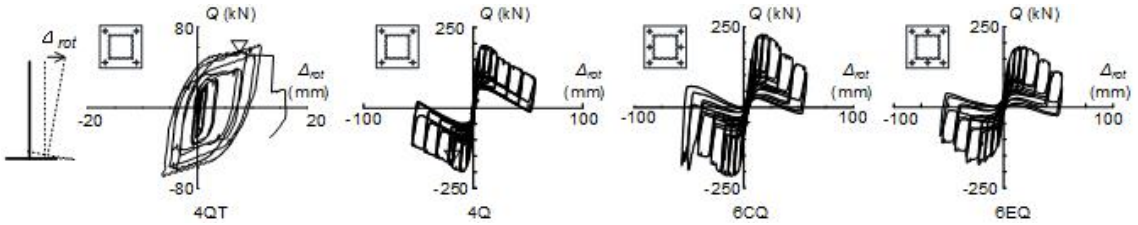

(b) shear force - column lateral displacement relationship

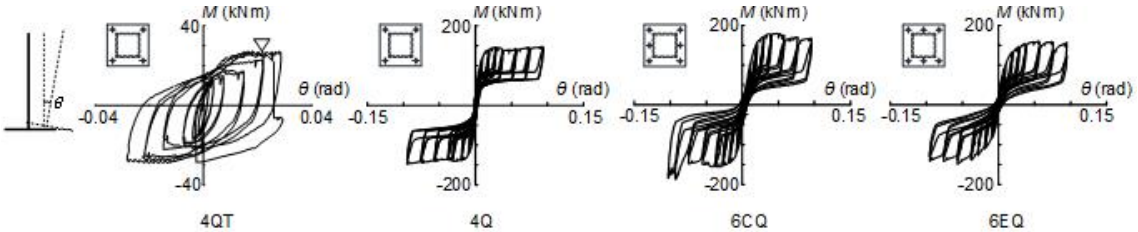

(c) Moment – column rotation angle relationship

Fig. 8 Hysteresis curves

on the anchor rods, the anchor rods in tension side yielded when the column rotation angle is around 0.02-0.03rad. As shown in Fig. 8(c), specimens reached the maximum moment when the column rotation is around 0.02-0.04 rad. However, the moment was nearly reduced in the following loading. Till the end of loading (0.1 rad column rotation angle), no anchor rods fractured for these three specimens.

The hysteresis curve of specimen 4Q and 6CQ were symmetrical in positive and negative loading. But the hysteresis curve of specimen 6EQ was unsymmetrical. It is because the two anchor rods were arranged in the column center line. The contribution of these two anchor rods in positive direction and negative direction is not the same, which will be discussed in the following section.

3.3 Backbone curves and energy dissipation

Backbone curves of the shear force and displacement of column top are compared in Fig. 9. Yield strength and maximum strength of the specimens are listed in Table 3.

When the axial force is 270 kN in tension (axial force ratio is -0.1), specimen 4QT yielded very early (0.005 rad column rotation angle). The moment of specimen 4QT was reduced by 70% because of the axial force changed from compressive 540 kN to tensile 270 kN. When the axial force is 540kN in compression (axial force ratio is 0.2), the maximum shear strength increased about 3 times compared with that of specimen 4QT. As the number of anchor rods increased, the column rotation angle of maximum strength was delayed to 0.03-0.04 rad (specimen 6CQ, 6EQ) from 0.02 rad (specimen 4Q).

Cumulative energy dissipations of each loading cycle for each specimen were illustrated in Fig.

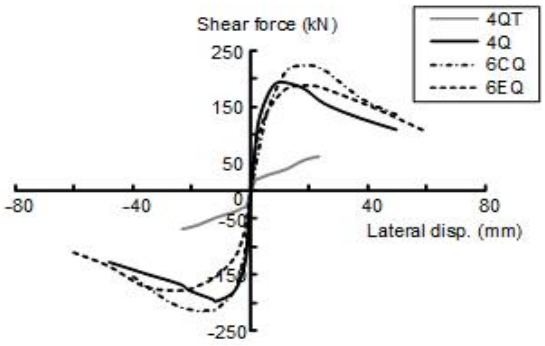

Fig. 9 Backbone curves

Table 3 Test results

Specimen	Yield			Maximum		
	Column rotation (rad)	*M* (kNm)	*Q* (kN)	Column rotation (rad)	*M* (kNm)	*Q* (kN)
4Q	0.005	12.7	21.6	0.04	28.1	65.2
4QT	0.02	137.8	195	0.02	147.4	195.7
6EQ	0.03	134.7	191.5	0.04	167.5	219.5
6CQ	0.02	117.4	160.4	0.03	154.3	183.5

10. Specimen 4QT showed the smallest energy dissipation capacity. The energy dissipation of specimen 4Q, 6CQ, and 6EQ were quite similar at the early loading stage (0.03 rad column rotation angle). After it, the anchor rods yielded, the energy dissipation of the specimens were different. Specimen 6CQ showed the most energy dissipation. It is mainly because that more anchor rods yielded and contributed to the shear resistance. Although specimen 6EQ have the same number of anchor rod with specimen 6CQ, the two anchor rods in the center line were not fully contribute to the shear resistance. Therefore, the energy dissipation was smaller than that of specimen 6CQ.

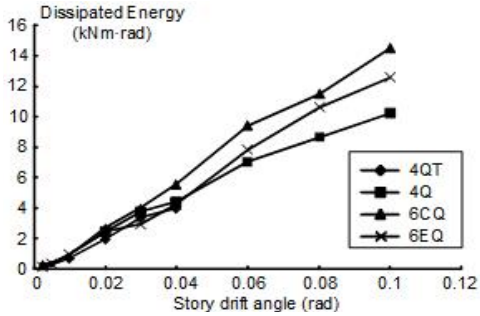

Fig. 10 Cumulative energy dissipation of each loading cycle

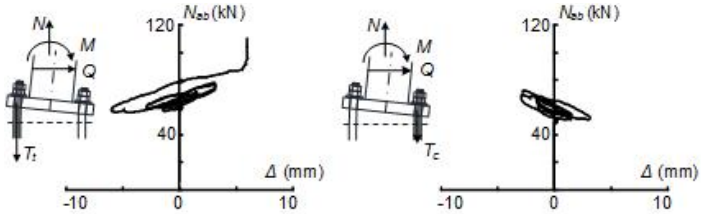

(a) Specimen 4QT

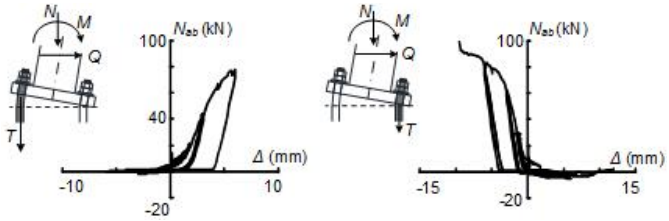

(b) Specimen 4Q

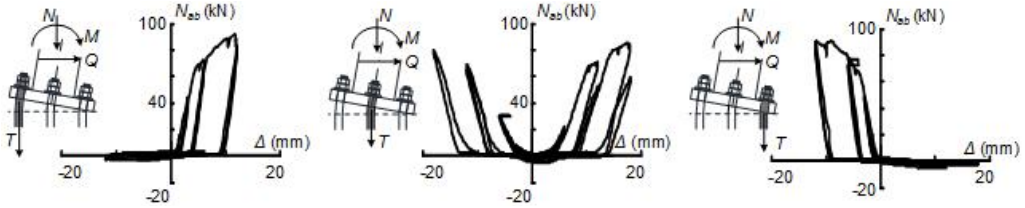

(c) Specimen 6EQ

Fig. 11 Tension of anchor rod - column rotation relationship

3.4 Effect of anchor rods

Strain gages were attached on the anchor rods as shown in Fig. 4(b). Therefore, the resistance mechanism of anchor rods could be discussed using these strain data. The relationship of anchor rod axial force and column rotation angle are shown in Fig. 11. The axial force of anchor rods were calculated using the recorded strain data.

As shown in Fig. 11(a), in specimen 4QT the axial force of anchor rods were tensile during the loading. For specimen 4QT, the axial force was tensile, and the base plate was separated from the mortar layer during the loading (Fig. 5).

For specimen 4Q (Fig. 11(b)), axial force of anchor rods were tensile only when the anchor rods were in the side which base plate separated from the mortar layer. When the base plate contacted with the mortar layer, the axial force of anchor rods was minimal.

For specimen 6EQ, there are two anchor rod in the center line of column along the loading direction, as shown in Fig. 11(c). It is noted that the behavior of these two anchor rods are different from the others. As shown in Fig. 11(c), the center two anchor rod resisted tensile axial force during the loading, but the behavior were different in positive and negative direction. It is because the rotation center of the base plate is at the center of anchor rods in compression side not the center of column. Therefore, as the base plate rotated, these two anchor rods were stressed in tension. And the axial force of these two anchor rods are smaller than the axial force of the anchor rods on the edge, since the deformation is smaller than those anchor rods. Therefore, the hysteresis curves of specimen 6EQ is not symmetry in positive and negative loading.

4. Strength estimation

The moment resistance of the exposed column base component is estimated by a moment couple that consists of the tension force in the anchor rods and the equivalent compressive force applied at the centroid of the bearing area under the base plate. The assumed stress distribution is shown in Fig. 12. Following the procedure adopted in standard design specification (AISC Design Guide No. 1 (Fisher and Koliber 2006); Architectural Institute of Japan (AIJ) 2006), the maximum strength, M_u, is estimated as

(1) When the anchor rods on the tension side take smaller forces than the yield strength $N_u \geq N$ $N_u - T_u$ (Fig. 12(a))

$$M_u = (N_u - N)d_t \tag{1}$$

(2) When the anchor rods on the compression side take tensile forces $-T_u \geq N > 2T_u$ (Fig. 12(c))

$$M_u = (N + 2T_u)d_t \tag{2}$$

(3) Otherwise $N_u - T_u \geq N > -T_u$ (Fig. 12(b))

$$M_u = T_u d_t + \frac{(N + T_u)D}{2}\left(1 - \frac{N + T_u}{N_u}\right) \tag{3}$$

where N = axial force transferred by the column base; N_u = maximum compressive strength of the

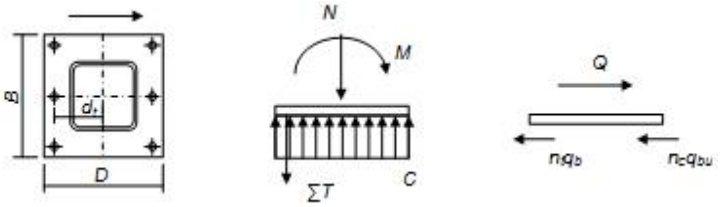

(a) $N_u \geq N > N_u - T_u$

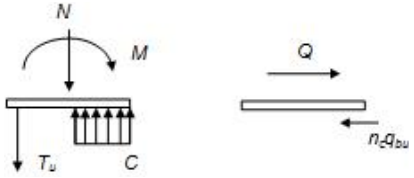

(b) $N_u - T_u \geq N > -T_u$

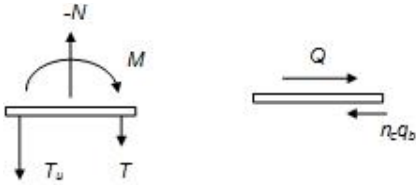

(c) $-T_u \geq N > -2T_u$

Fig. 12 Model of evaluation of the maximum moment and shear force resisted by exposed column base

concrete under the base plate, estimated as $0.85BDf_c$'; T_u = maximum tensile strength of the anchor rods acting in the tension region; and f_c' = compressive strength of concrete in the foundation. Other geometric notations are defined in Fig. 12.

The shear resistance of exposed column base is estimated by the maximum value of the friction resistance, Q_{fu}, induced by the moment resistance and the shear bearing of anchor rods, Q_{bu}.

$$Q_u = \max(Q_{fu}, Q_{bu}) \tag{4}$$

(1) When the anchor rods on the tension side take smaller forces than the yield strength $N_u \geq N > N_u - T_u$ (Fig. 12(a))

$$Q_{fu} = 0.5N \tag{5}$$

$$Q_{bu} = n_c \cdot q_{bu} + n_t \cdot q_{bu} \sqrt{1 - \left(\frac{N_u - N}{T_u} \right)^2} \tag{6}$$

(2) When the anchor rods on the compression side take tensile forces $-T_u \geq N > -2T_u$ (Fig. 12(c))

$$Q_{fu} = 0.5\left(N + T_u\right) \tag{7}$$

$$Q_{bu} = n_c \cdot q_{bu} \tag{8}$$

Table 4 Comparison of test and calculated results

Specimen	Max. moment (kNm)			Max. shear strength (kN)		
	Test	Calculation	Cal./Test	Test	Calculation	Cal./Test
4QT	28.14	36.1	1.28	65.2	157.8	2.42
4Q	147.4	150.4	1.02	195.6	406.7	2.08
6EQ	154.34	176.1	1.14	183.5	543.3	2.96
6CQ	167.5	181.6	1.08	219.5	475	2.16

(3) Otherwise $N_u - T_u \geq N > -T_u$ (Fig. 12(b))

$$Q_{fu} = 0 \tag{9}$$

$$Q_{bu} = n_c \cdot q_{bu} \sqrt{1 - \left(\frac{-N - T_u}{T_u} \right)^2} \tag{10}$$

where N = axial force transferred by the column base; N_u = maximum compressive strength of the concrete under the base plate, estimated as $0.85BDf_c'$; T_u = maximum tensile strength of the anchor rods acting in the tension region; n_c = the number of anchor rods on the compression side; n_t = the number of anchor rods on the tension side; and q_{bu} = maximum shear resistance of single anchor rod.

The comparison between test and calculated results are shown in Table 4. It is noted that the moment resistance was evaluated well using the equations provided by the design manual. The difference between evaluated and test moment strength is around 10% for the specimens under compressive axial load. However, the difference between evaluated and test moment strength is 30% for the specimen under tensile axial load. The shear resistance was not be evaluated well. It is note that the differences between test results and calculated results using design manual equations are quite large, which are 2-3 times test results.

As shown in Fig. 7(b), when the tensile axial load was applied, the base plate and mortar layer could be separated. Therefore, the contribution of friction force was zero, anchor rods bearing will contribute to the shear transfer. However, the stress condition of anchor rod would be critical. Anchor rods would resist tension, shear, and moment simultaneously. The anchor rod capacity would be significantly reduced under such critical stress condition. And slip between base plate and mortar layer was significant large, which was observed in this test and previous braced exposed column base test (Cui *et al*. 2015). Therefore, the evaluation of both moment and shear strength for the exposed column base connections under tensile axial force should be revised by considering the complex stress condition.

5. Conclusions

Based on the quasi-static cyclic loading test, the seismic behavior of exposed column base under different axial load was investigated. Test variables were the axial force level, the number of anchor rods, and the arrangement of anchor rods. Major observations obtained from this study are as follows.

- The load condition of column base is quite complex, the rotation and slip of column base always occurred simultaneously. Depends on the ratio of axial force and shear force, the shear resisting mechanism could be rotation type and slip type.
- When the axial force is compression, the shear force will be resisted by the friction between base plate and mortar layer. Furthermore, the moment resisted by the exposed column base would contribute to the shear resisting mechanism.
- The bending moment resistance of exposed column base increased as the number of anchor rods increased. When the number of anchor rod increased from 4 to 6, the resisted moment and dissipated energy increased by 12% and 20%, respectively.
- The hysteresis behavior of exposed column base will be different when the arrangement of anchor rods changed. The resisted moment will be increased, when the anchor rods were arranged further from the center line of column.
- When the axial force is tension, the friction force between base plate and mortar layer was overcome, the slippage of base plate will be relatively large. The shear force will be resisted by the anchor rods directly, and the strength was reduced significantly.
- When the axial force is compression, the exposed column base connection will develop additional resistance from friction that would develop from clamping action which arises when the base plate displaces laterally leading to increased tension forces in the anchor rods. To ensure the column base seismic behavior, the uplift of base plate is suggested to avoid.
- The evaluation method provided in the design code could estimate the moment resistance with acceptable tolerance for the specimen under compression axial load. Further study should be conducted to improve the evaluation of both moment and shear resistance of exposed column base under tensile axial load.

Acknowledgments

The research described in this paper was financially supported by the National Science Fund of China (51208076) and the Fundamental Research Funds for the Central Universities (DUT14LK04).

References

Ai, W., Tong, G., Zhang, L., Gan, G. and Shen, J. (2012), "Experimental study of shear behavior of anchor bolt connections at steel column bases", *J. Build. Struct.*, **33**(3), 80-88.

Akiyama, H. (1985), *Seismic Design on Column Bases of Steel Structures*, Gihodo Press, Tokyo, Japan.

American Institute of Steel Construction (AISC) (2005a), Seismic Provisions for Structural Steel Buildings, Chicago, IL, USA.

American Institute of Steel Construction (AISC) (2005b), Steel Construction Manual, Chicago, IL, USA.

Architectural Institute of Japan (AIJ) (2006), Recommendations for design of connections in steel structures; Tokyo, Japan.

Astaneh, A., Bergsma, G. and Shen, J.H. (1992), "Behavior and design of base plates for gravity, wind and seismic loads", *Proceedings of the National Steel Construction Conference*, Las Vegas, NA, USA, June.

Borzouie, J., MacRae, G.A., Chase, J.G., Rodgers, G.W. and Clifton, G.C. (2016), "Experimental studies on cyclic performance of column base strong axis-aligned asymmetric friction connections", *J. Struct. Eng., ASCE*, **142**(1), 04015078.

Burda, J.J. and Itani, A.M. (1999), "Studies of seismic behavior of steel base plates", Report No. CCEER

99-7; Center for Civil Engineering Earthquake Research, Department of Civil Engineering, Universtiy of Nevada, Reno, NA, USA.
Burdette, E.G., Perry, T.C. and Funk, R.R. (1987), *Test of Undercut Anchors*, ACI Special Publication SP-103.
Chi, H. and Liu, J. (2012), "Seismic behavior of post-tensioned column base for steel self-centering moment resisting frame", *J. Constr. Steel. Res.*, **78**, 117-130.
Cook, R.A. and Klingner, R.E (1992), "Behavior of multiple-anchor steel-to-concrete connections with surface mounted baseplates", *Anchors in Concrete – Design and Behavior SP*, *ACI*, **130**, 61-122.
Cui, Y., Nagae, T. and Nakashima, M. (2009), "Hysteretic behavior and strength capacity of shallowly embedded steel column bases", *J. Struct. Eng.*, *ASCE*, **135**(10), 1231-1238.
Cui, Y., Kishiki, S. and Yamada, S. (2015), "Seismic behavior of braced frame column base connections", *Behavior of Steel Structures in Seismic Areas* (*STESSA2015*), Shanghai, China, July.
Demir, S., Husem, M. and Pul, S. (2014), "Failure analysis of steel column-RC base connections under lateral cyclic loading", *Struct. Eng. Mech.*, *Int. J.*, **50**(4), 459-469.
DeWolf, J.T. (1982), "Column base plates", *Struct. Eng. Practice*, **1**:**1**, 39-51.
European Committee for Standardization (CEN) (1992), ENV 1993 Eurocode 3; Design of steel structures, Brussels, Belgium.
Fisher, J.M. and Kloiber, L.A. (2006), *Base Plate and Anchor Rod Design*, (2nd Edition), Steel Design Guide Series No. 1, AISC, Chicago, IL, USA.
Grauvilardell, J.E., Lee, D., Ajar, J.F. and Dexter, R.J. (2005), "Synthesis of design, testing and analysis research on steel column base plate connections in high seismic zones (ST-04-02)", Department of Civil Engineering, University of Minnesota, Minneapolis, MN, USA.
Japanese Society of Steel Construction (JSSC) (2009), Recommendation and Commentary for Construction of Exposed Column Base with Structural Anchor Bolts, Tokyo, Japan.
Kanvinde, A.M., Grilli, D.A. and Zareian, F. (2012), "Rotational stiffness of exposed column base connections: experiments and analytical models", *J. Struct. Eng.*, *ASCE*, **138**(5), 549-560.
Kanvinde, A.M., Higgins, P., Cooke, R.J., Perez, J. and Higgins, J. (2015), "Column base connections for hollow steel sections: seismic performance and strength models", *J. Struct. Eng.*, *ASCE*, **141**(7), 04014171.
Nagae, T., Ikenaga, M., Nakashima, M. and Suita, K. (2006), "Shear friction between base plate and base mortar in exposed steel column base", *J. Struct. Construct. Eng.*, *Architect. Inst. Japan*, **606**, 217-223.
Rabbat, B.G. and Russel, H.G (1985), "Friction coefficient of steel on concrete or grout", *J. Struct. Eng.*, *ASCE*, **111**(3), 505-515.
Rotz, J.V. and Reifschneider, M. (1989), "Combined axial and shear load capacity of embedments in concrete", *Proceedings of the 10th Conference on Structural Mechanics in Reactor Technology*, Anaheim, CA, USA.
Sato, K. (1987), "A research on the aseismic behavior of steel column base for evaluating its strength capacity and fixity", Report No. 69; Kajima Institute of Construction Technology, Tokyo, Japan.
Stamatopoulos, G.N. and Ermopoulos, J.C. (2011), "Experimental and analytical investigation of steel column bases", *J. Constr. Steel. Res.*, **67**(9), 1341-1357.
Thambiratnam, D.P. and Paramasivam, P. (1986), "Base plate under axial loads and moments", *J. Struct. Eng.*, *ASCE*, **112**(5), 1166-1181.
Xiao, N., Li, S. and Zhao, W. (2010), "Calculation of shear capacity of shear connector in steel column base", *J. Build. Struct.*, **31**(7), 86-93.

CC